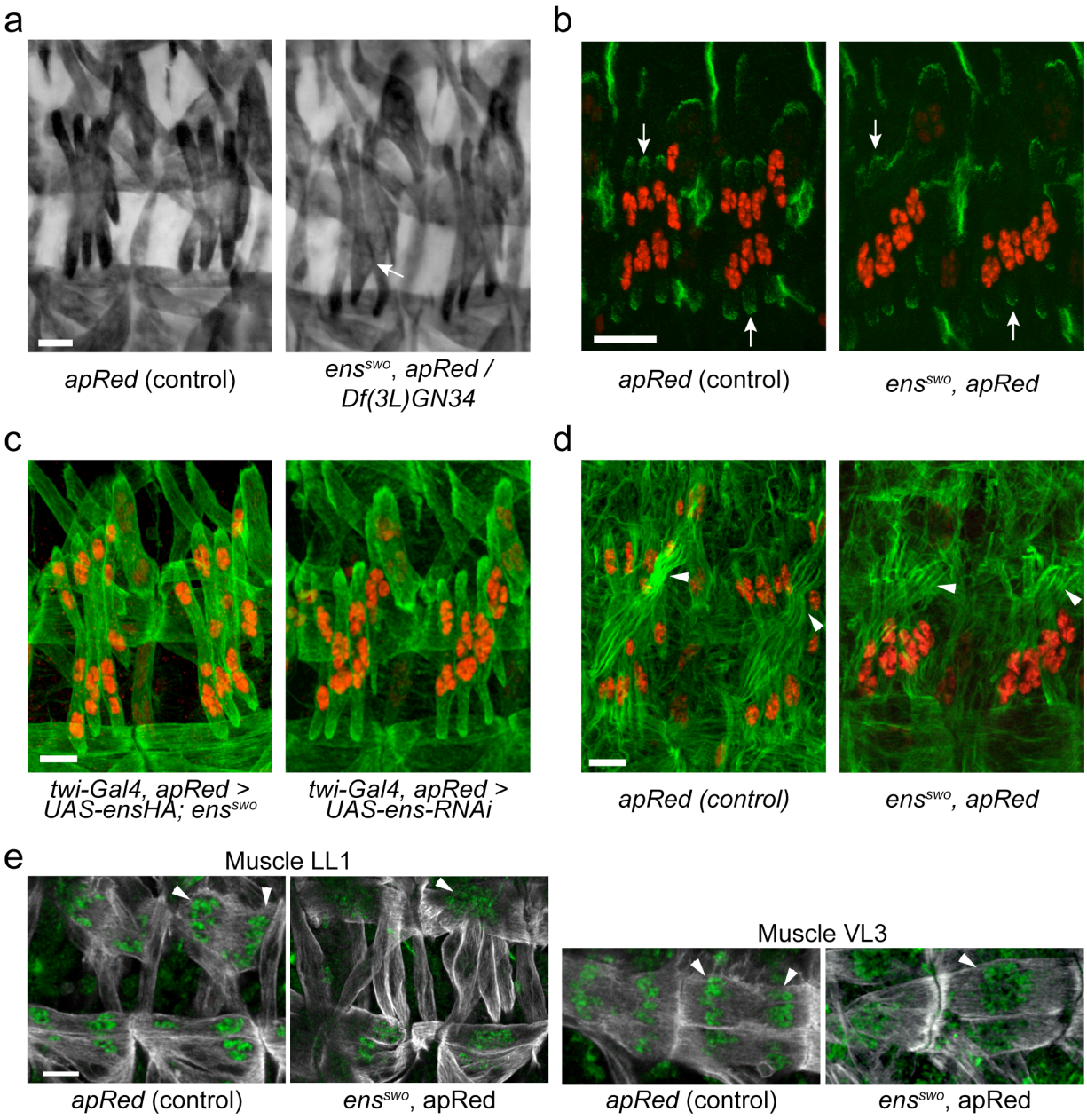

Supplementary Figure 1

Supplementary Figure 1 | Loss of Ensconsin/MAP7 affects nuclear positioning but not muscle elongation or attachment. a, Two representative hemi-segments from stage 16 *apRed* (control) and *ens^{swo}* mutant embryos immunostained to reveal the muscle pattern (anti-Tropomyosin). The mutant contains the *ens^{swo}* allele over a deficiency that removes *ens*. The *ens^{swo}* phenotype is 100% penetrant. The arrow identifies the ventral bulge created in the myotube by the clustered nuclei. Bar, 10μm. **b**, Two representative hemi-segments from stage 15 *apRed* (control) and *ens^{swo},apRed* mutant embryos labeled with antibodies against β-PS Integrin (green) and dsRed (red). Arrows indicate normal accumulation of β-PS Integrin at the ends of the muscles at muscle attachment sites in *ens^{swo},apRed* mutant embryos. Bar, 20μm. **c**, Two representative hemi-segments from stage 16 embryos labeled with antibodies against Tropomyosin (green) and dsRed (red). The left images show the position of nuclei in *twist-Gal4>UAS-ensHA;ens^{swo}* embryo in which Ens is expressed in the developing mesoderm and muscle, while the right image shows the effect upon nuclear position of *twist-Gal4>UAS-ens-RNAi* in a wild-type embryo. These data reveal that Ens is required in muscle for proper nuclear positioning. Bar, 10μm. **d**, Two representative hemi-segments from stage 16 embryos immunostained for α-Tubulin (green) and dsRed (red). Arrowheads indicate the MT rich chordotonal organs overlying the muscles. MT organization appears normal in *ens^{swo},apRed* mutants. Bar, 10μm. **e**, Lateral view of 2 hemi-segments from stage 16 *apRed* (control) and *ens^{swo},apRed* mutant embryos immunostained for Vestigial (green) and Tropomyosin (white). Arrowheads highlight the nuclei in muscle LL1 and muscle VL3. Nuclei are mispositioned in all muscles analyzed in the *ens^{swo},apRed* mutant. Bar, 10μm.

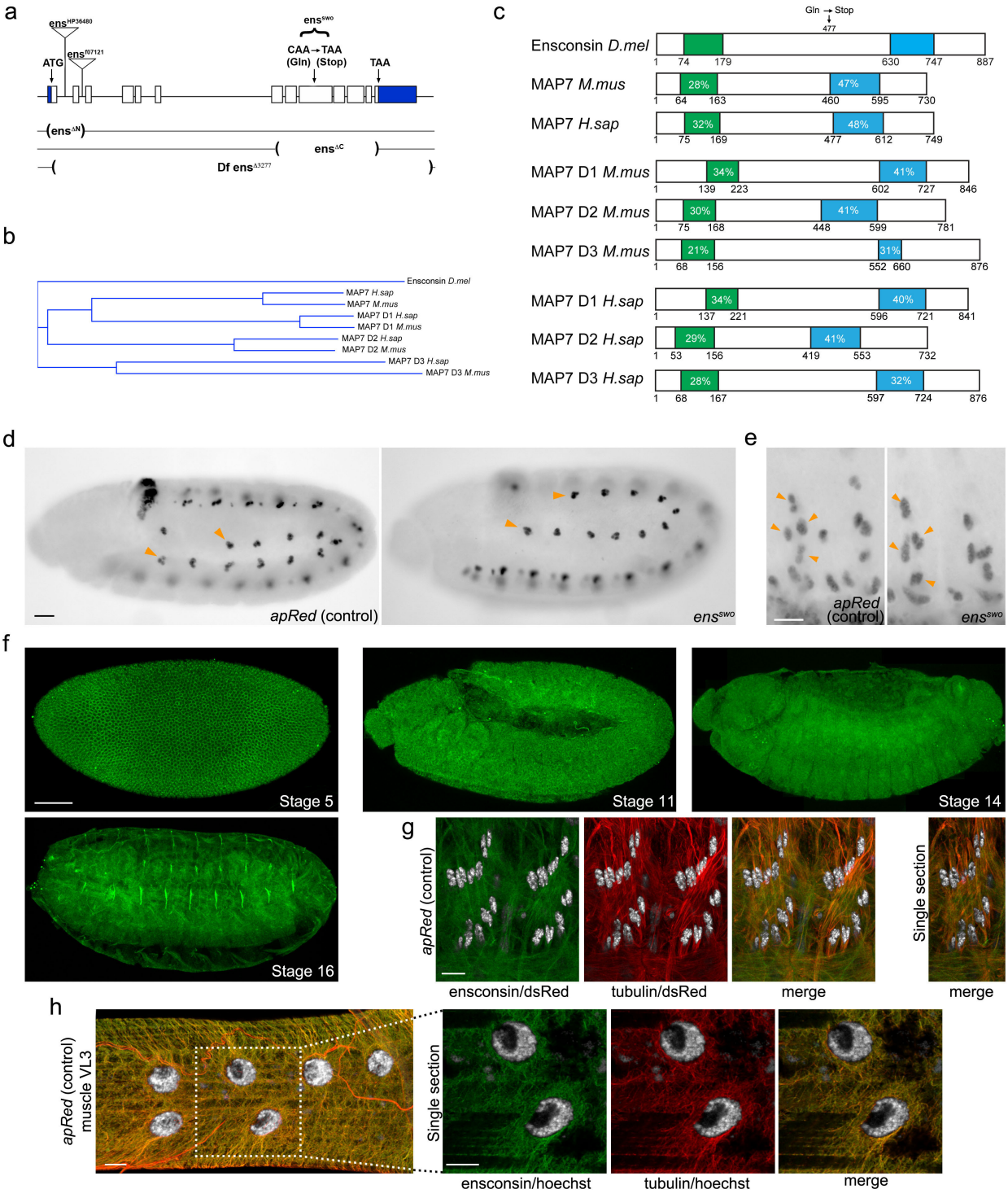

Supplementary Figure 2

Supplementary Figure 2 | Ensconsin/MAP7 is conserved from flies to mammals and is widely expressed throughout development. a, Schematic diagram of the *ens* locus in *Drosophila*. The genomic disruption present in each *ens* allele used for this study is indicated: EMS allele (CAA to TAA), P-element alleles (triangles), deletion alleles (bar with parenthesis)[9]. ens^{swo} failed to complement all indicated alleles of *ens* and the phenotype of homozygous ens^{swo} mutants was indistinguishable from $ens^{swo}/Df(3L)GN34$ that removes a region including the entire *ens* locus, suggesting that ens^{swo} is a null allele or strong hypomorph. **b**, Phylogenetic tree showing the evolutionary relationship between the amino acid sequences of *Drosophila*, mouse and human MAP7 families. **c**, Schematic diagrams of *Drosophila* Ens, mouse and human MAP7 family proteins. Alignment of D.mel Ens (Q9I7T2) with human MAP7 (Q14244) using NCBI/ Blast/blastp determined consensus sequences between the proteins. Two domains from Ens (Domain 1, green, aa74 to 179; Domain 2, blue, aa630 to 747) were aligned to human and mouse MAP7 family proteins using the LALIGN program (http://www.ch.embnet.org/software/LALIGN_form.html). Consensus regions (blue and green boxes) include the percentage of identity for the region and amino acid position. **d**, Stage 11 *apRed* (control) and ens^{swo},*apRed* mutant embryos immunostained for Even-skipped. Arrowheads mark the ends of the U shape row of founder cells. Eve Founder cells are specified normally in ens^{swo},*apRed* mutant embryos. Bar, 20µm. **e**, Two hemi-segments from early stage 14 *apRed* (control) and ens^{swo},*apRed* mutant embryos immunostained for Krüppel indicate founder cell specification of a different subset of muscles is normal in ens^{swo},*apRed* mutants. Krüppel labels a subset of founder cells within a single hemi-segment (a different subset of muscles than are labeled by Eve). Arrowheads mark 4 pairs of cells in a single hemi-segment showing the presence of the founder cells for LL1, LT2, LT4, and VA2 that have each undergone an initial fusion event. Bar, 10µm. **f**, Representative maximum intensity projection images of embryos immunostained for Ens at progressive stages of development. Ens is broadly expressed during embryonic development. Bar, 50µm. **g**, A maximum intensity projection of two hemi-segments from a stage 16 *apRed* (control) embryo immunostained for Ens (green), dsRed labeled nuclei (white), and α-tubulin (red). The single hemi-segment is one optical section taken from the stack used to produce the maximum intensity projections. Ens and MT show overlapping expression. Bar, 10µm. **h**, A maximum intensity projection of a portion of muscle VL3 from segment A3 of an *apRed* (control) L3 larva stained with Hoechst (white) to reveal nuclei and immunostained for Ens (green), and α-tubulin (red). The white box identifies the area where higher magnification reveals co-expression of Ens and MT. These images also reveal MT organization around nuclei. Bar, 10µm.

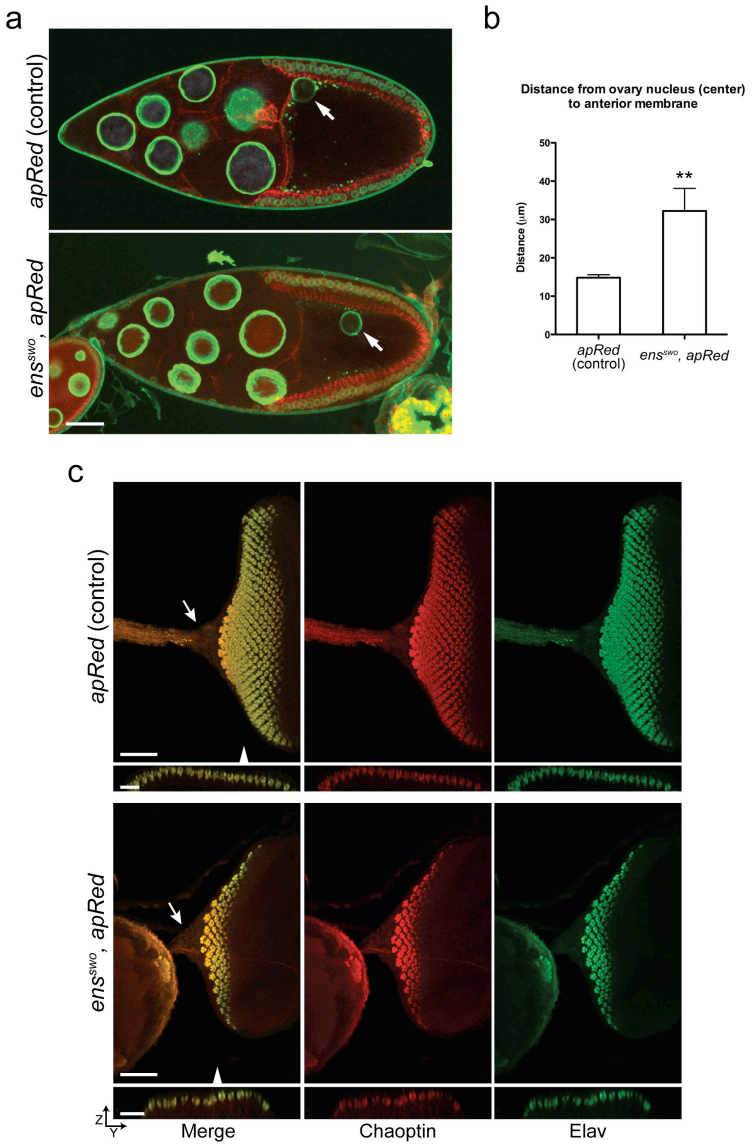

Supplementary Figure 3 | Nuclei are mispositioned in oocytes but not in photoreceptor cells. **a**, Stage 10 egg chambers from *apRed* (control) and *ens*^{swo} mutant female ovaries stained with wheat germ agglutinin (green) to label the nuclear envelope and phalloidin (red) to label F-actin. Nuclei in *ens*^{swo} mutant oocytes are mispositioned and do not localize to the anterior edge of the developing oocyte. Bar, 15 µm **b**, Histogram of nuclear position in *apRed* and *ens*^{swo} mutant oocytes. Error Bars, s.e.m. **p < 0.01. **c**, Eye discs from *apRed* and *ens*^{swo} mutant wandering L3 larvae immunostained for Elav to label photoreceptor cell nuclei (green) and for Chaoptin to label photoreceptor cell membranes (red). Arrowhead indicates position of YZ image, which shows that all photoreceptor cell nuclei are apically localized and aligned adjacent to each other in both control and mutant eye discs. Additionally, no nuclei are found in the optic stalk (arrow). Bar (XY), 30 µm. Bar (YZ), 15 µm.

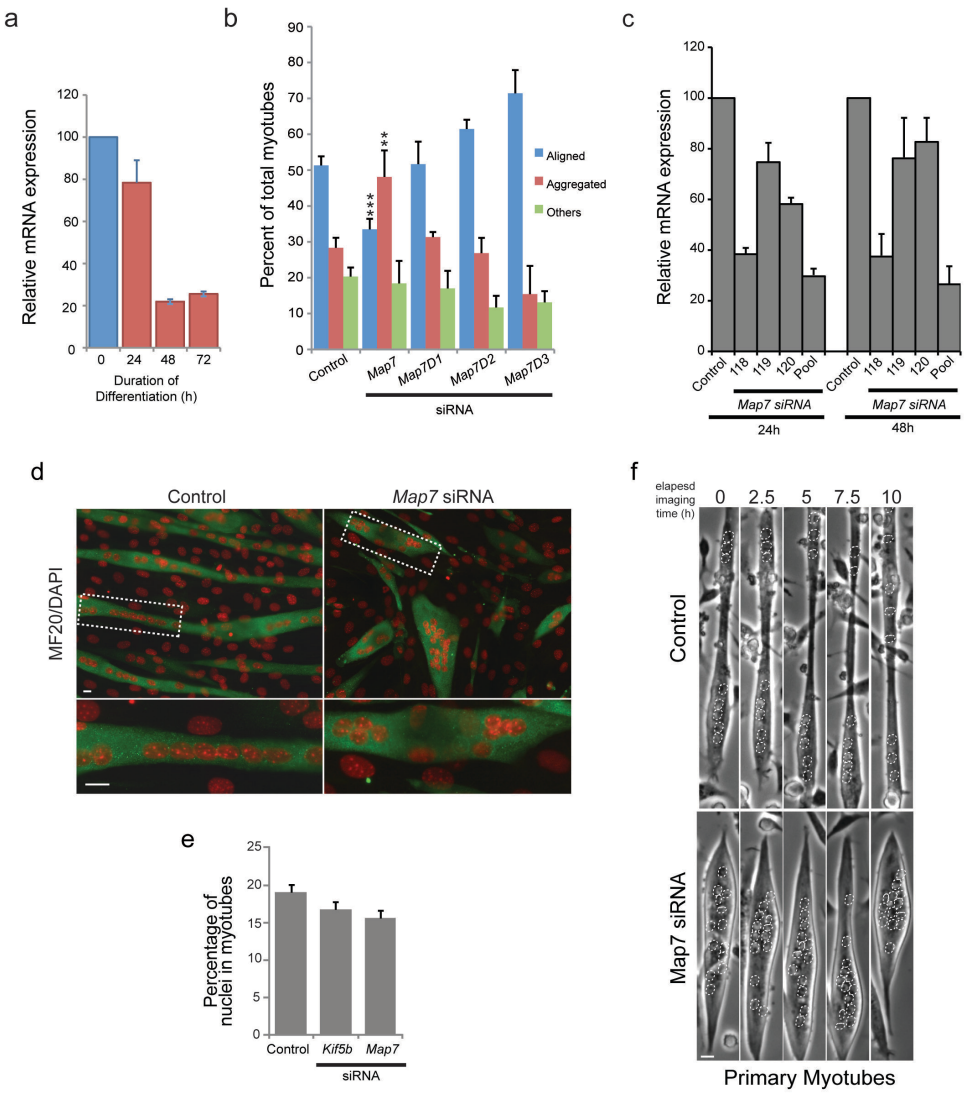

Supplementary Figure 4 | MAP7 expression in mammalian myotubes. a, Relative expression of Map7 mRNA from C2C12 myoblasts at different time points of differentiation. Relative expression levels were quantified using qPCR. Error Bars, s.e.m. **b**, Histogram of nuclear distribution in C2C12 myotubes from untreated (control) and *Map7* family siRNA pool treated cells. Error Bars, s.e.m. ***$p < 0.001$, **$p < 0.01$ (control vs. experimental condition) **c**, Relative expression of *Map7* mRNA in C2C12 cells 24h or 48h after no transfection (control) or transfection with individual *Map7* siRNAs or *Map7* siRNA pool. Relative expression levels were quantified using qPCR. Error Bars, s.e.m. **d**, Representative immunofluorescence images of C2C12 myotubes untreated (control) or *Map7* siRNA pool treated (*Map7* siRNA), differentiated for 4 days and immunostained for MHC (green) and DAPI (red). Bar, 15 µm. **e**, Histogram of fusion index in C2C12 myotubes untreated (control), *Kif5b* siRNA pool or *Map7* siRNA pool, differentiated for 4 days. More than 400 nuclei were scored in each experiment. Error Bars, s.e.m. The difference is not significant, $p > 0.25$. **f**, Images from a representative time-lapse phase contrast movie of primary myotubes in untreated (control) or *Map7* siRNA pool treated cells. Outlines indicate the position of nuclei. Bar, 15 um.

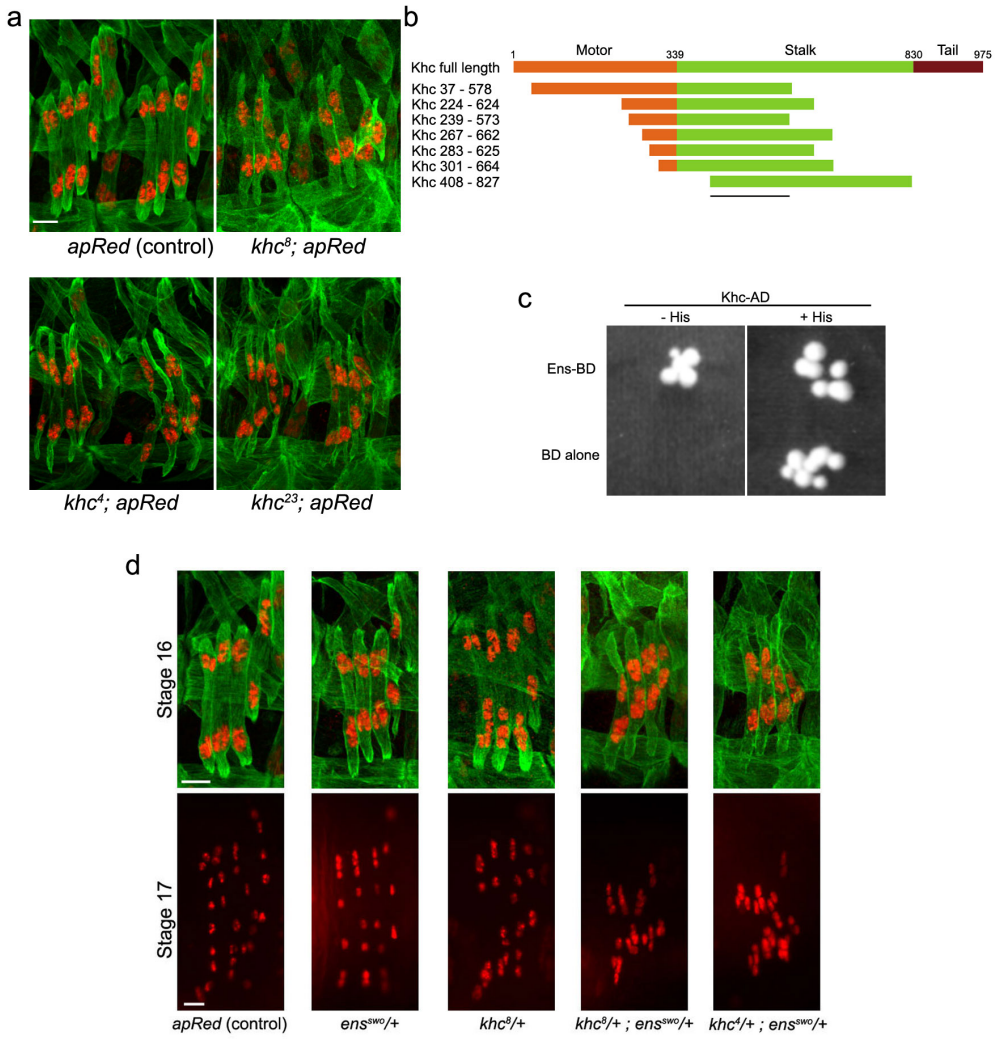

Supplementary Figure 5 | Analysis of the role of different domains of Kinesin on nuclear positioning. **a**, Representative immunofluorescent images of 2 hemi-segments from stage 16 *apRed* (control) and *khc,apRed* mutant embryos immunostained to reveal muscle (anti-Tropomyosin; green) and nuclei (dsRed; red). *khc*^{8} is a null allele[12], while khc^{4} and khc^{23} each have specific point mutations within the motor domain of kinesin[12]. Bar, 10µm. **b**, Schematic diagram of the Khc protein and the fragments of Khc that interacted with Ens in a yeast 2-hybrid screen. Numbers indicate positions on the primary amino acid sequence, while the black bar identifies the region within the Kinesin stalk domain that is common to all of these forms of Khc. This region is common to all fragments suggesting that Ens interacts with stalk domain of Khc. **c**, Representative results from the yeast 2-hybrid screen where full-length Khc, fused to the activation domain (AD) of Gal4, interacts with full length Ens fused to the DNA binding domain (BD) of Gal4 to drive expression of the auxotrophic marker His. +His plates are supplemented with His as a positive control, while –His plates lack this essential amino acid. **d**, Single hemi-segments from stage 16 (15h AEL) and stage 17 (18h AEL) embryos of the indicated genotypes. Stage 16 embryos were fixed and immunostained for muscle (tropomyosin, green) and nuclei (dsRed, red). apRed (red) was imaged live in late stage 17 embryos. Bar, 10µm.

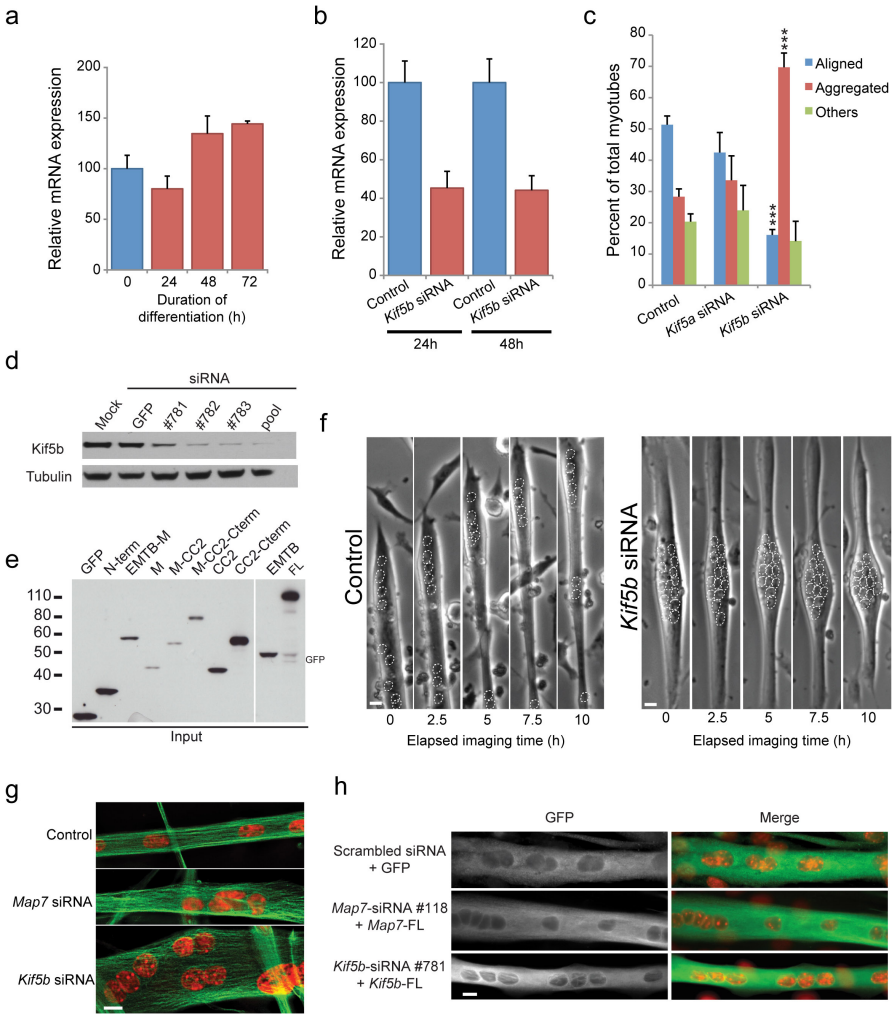

Supplementary Figure 6 | Kif5b expression in mammalian myotubes. a, Relative expression of *Kif5b* mRNA from C2C12 myoblasts at different time points of differentiation. Relative expression levels were quantified using qPCR. Bars, s.e.m. **b**, Relative expression of *Kif5b* mRNA in C2C12 cells 24h or 48h after no transfection (control) or transfection with *Kif5b* siRNA pool. Relative expression levels were quantified using qPCR. Error bars, s.e.m. ***p <0.001. **c**, Histogram of nuclear distribution in C2C12 myotubes from control, *Kif5a*, and *Kif5b* siRNA treated cells. Error Bars, s.e.m. ***p < 0.001. **d**, Western blot for Kif5b of C2C12 cell lysates 3 days after no transfection (control) or transfection with GFP, *Kif5b* siRNAs (#781, #782 and #783) or *Kif5b* siRNA pool. **e**, Western blot for GFP of C2C12 cells lysates expressing GFP-MAP7 constructs (see Figure 3 for constructs). **f**, Images from a representative time lapse phase contrast movie of primary myotubes in untreated (control) or *Kif5b* siRNA pool treated cells. Outlines indicate the position of nuclei. Bar, 15 um. **g**, Representative immunofluorescence images of primary myotubes untreated (control), *Map7* siRNA pool treated or *Kif5b* siRNA pool treated, differentiated for 3 days, and immunostained for α-tubulin (green) and DAPI (red). Bar, 15 μm. **h**, Representative immunofluorescence images of myotubes treated with the indicated siRNA sequences and expressing the indicated constructs and immunostained for GFP (green) and DAPI (red). Bar, 15 um.

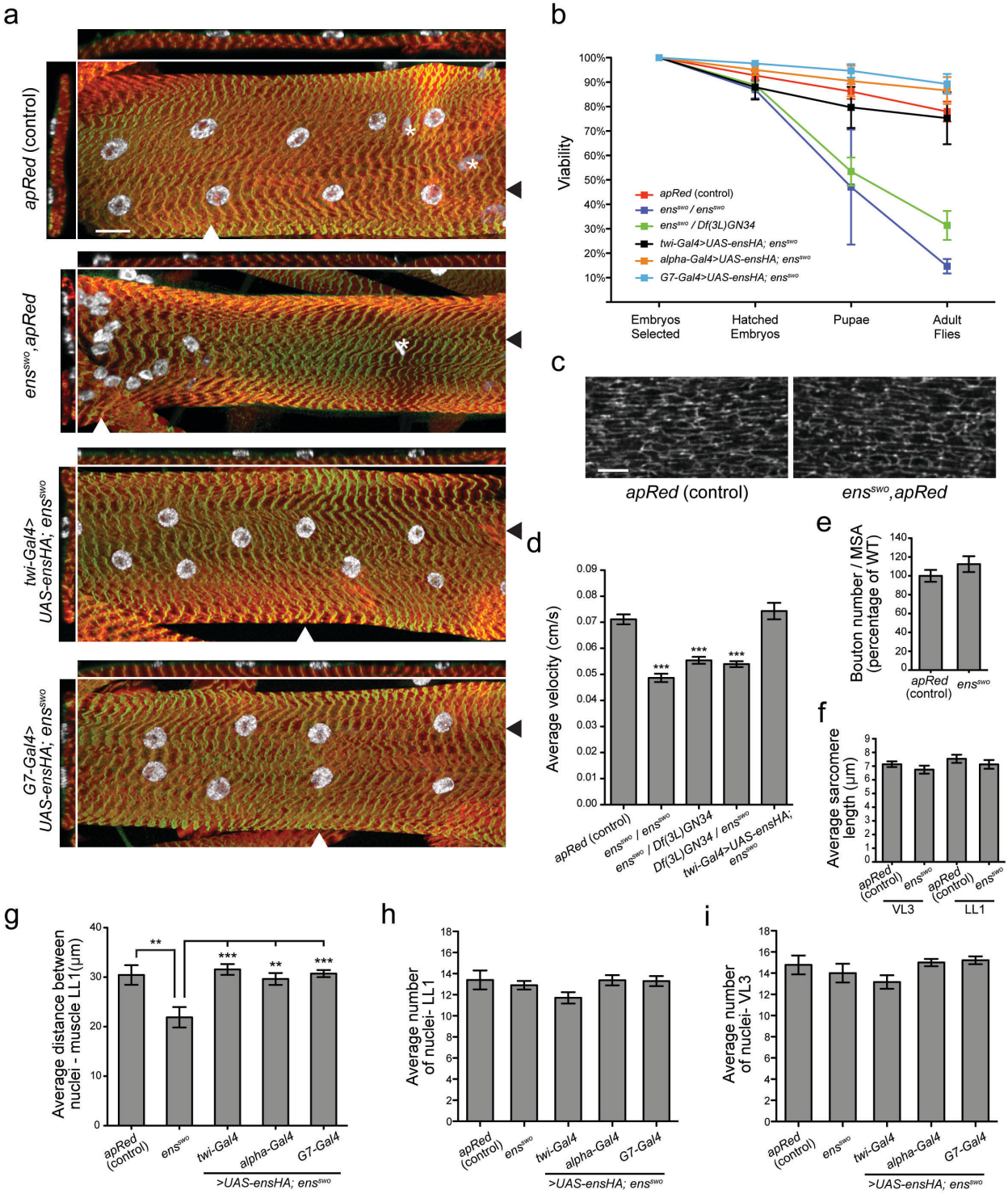

Supplementary Figure 7

Supplementary Figure 7 | Loss of ensconsin/MAP7 affects nuclear positioning in different muscle types. a, L3 larvae were dissected, fixed and stained with phalloidin (red) and Hoechst (white) and immunostained to reveal Z-bands (anti-Zasp; green). Maximum intensity XY projections with single XZ (shown top, indicated by black arrowhead) and YZ (shown left, indicated by white arrowhead) slices from a confocal stack of muscle LL1 from segment A3 of L3 larvae from the indicated genotypes are shown. Stars (*) mark nuclei in neurons lying on the surface of the muscle, or nuclei from underlying muscles. Bar, 20 μm. **b**, Quantification of the viability of the indicated genotypes throughout the various stages of fly development. Error bars: s.e.m. **c**, Single confocal sections of a portion of muscle VL3 from *apRed* (control) and ens^{swo}, *apRed* mutant larvae immunostained with an antibody against Discs Large that labels the transverse tubule (t-tubule network). T-tubule morphology appears unaffected in *ensconsin* mutants. Bar, 5 μm. **d**, Histogram of the mean velocity of migration for L3 larvae of the indicated genotypes. Here, the locomotion of homozygous ens^{swo} mutants is impaired to a similar degree as are larvae carrying one allele of ens^{swo} over the deficiency that removes the *ens* locus. Additionally, this impairment is not affected by the sex of the parent that contributed the allele (the allele from the female is listed first to the left of the backslash and the male donated allele is listed after). Expression of *UAS-ensHA* in ens^{swo} mutants using *twist-Gal4* rescues the locomotive defect. Error bars, s.e.m. ***$p < 0.001$. **e**, Quantification of the bouton number for muscle 4 (LL1) in segment A3, normalized for muscle surface area (MSA), in *apRed* (control) and ens^{swo},*apRed* mutant larvae. Error bars, s.e.m. Difference is not significant, $p > 0.1$. **f,** Histogram of the average sarcomere length in control (*apRed*) and *ens* mutant L3 larvae for muscles LL1 and VL3. Error bars, s.e.m. The difference is not significant, $p > 0.25$. **g,** Histogram of the nearest neighbor analysis of nuclei within muscle LL1 from segment A3 from L3 larvae of the indicated genotype. Error bars, s.e.m. ***$p < 0.001$, **$p < 0.01$. **h,** Histogram of the average number of nuclei in muscle LL1 of segment A3 from L3 larvae of the indicated genotypes. There is no significant difference ($p > 0.25$) between the average number of nuclei in the control (13.4) and the other genotypes. Error bars, s.e.m. **i,** Histogram of the average number of nuclei in muscle VL3 of segment A3 from L3 larvae of the indicated genotypes. There is no significant difference ($p > 0.16$) between the average number of nuclei in the control (14.9) and the other genotypes. Error bars, s.e.m.

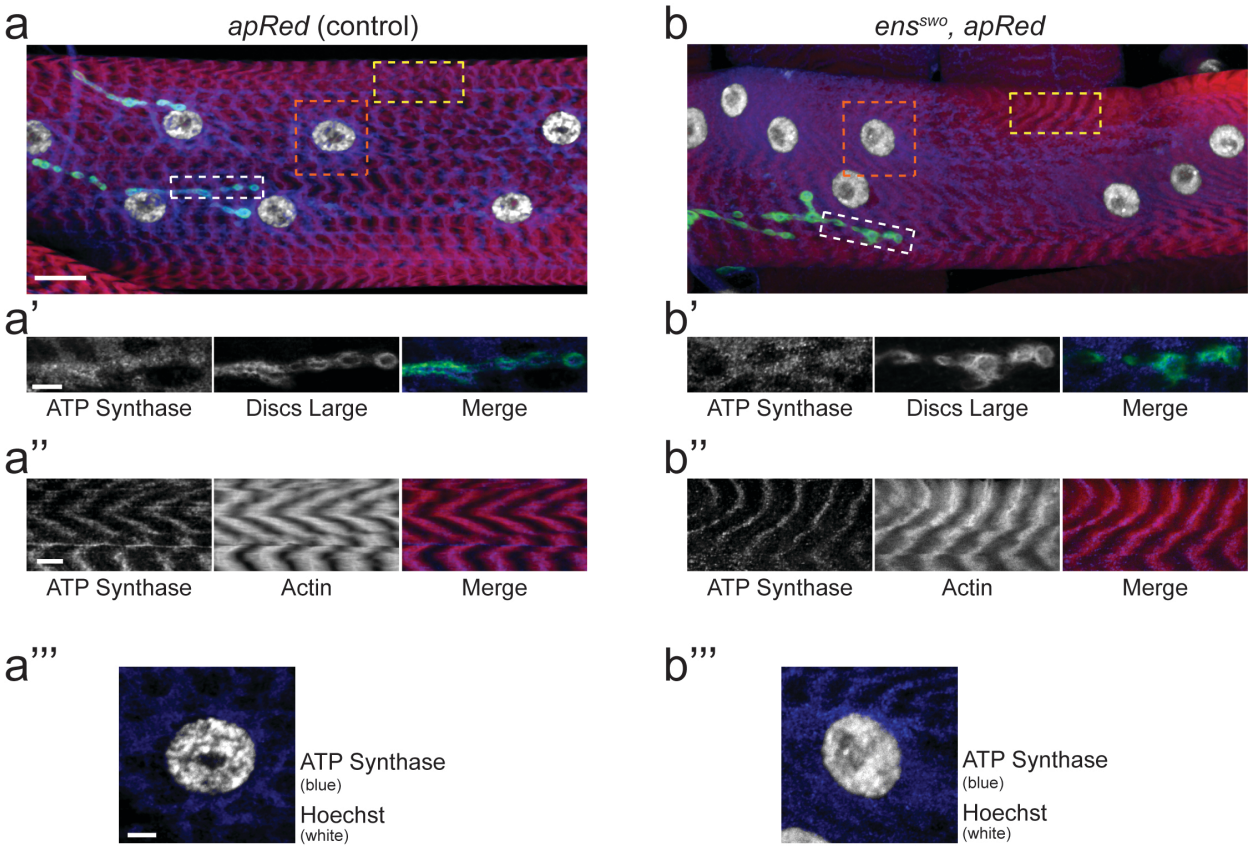

Supplementary Figure 8 | Mitochondria localize properly in *ens* mutant muscles. **a-b**, Maximum intensity projections from confocal images of muscle LL1 in *apRed* (control) and *ens*^{swo} mutant L3 larvae immunostained for mitochondria (ATP synthase, blue), post-synaptic membrane (Discs Large; green), sarcomeres (F-actin: phalloidin; red) and nuclei (Hoechst; white). White boxes identify regions magnified in **a'** and **b'**, yellow boxes indicate the regions magnified in **a"** and **b"**, and orange boxes indicate the regions magnified in **a"'** and **b"'**. Bar, 20 µm. Nuclei in the *ens*^{swo} mutant muscle cluster and do not align in two evenly spaced rows as observed in the control. **a'-b'**, Single confocal sections of the boxed area (white) in **a** and **b**. Bar, 5 µm. Mitochondria accumulate at the post-synaptic membrane of the neuromuscular junction indicated by the co-localization of ATP synthase and Discs Large (merge). **a"-b"**, Single confocal sections of the boxed area (yellow) in **a** and **b**. Mitochondria accumulate in the sarcomeres as indicated by the overlap of ATP synthase and phalloidin. Bar, 5 µm. **a"'-b"'**, maximum intensity projection of a 1.2 µm thick region of the boxed area (orange) in **a** and **b**. Mitochondria (blue) accumulate around the nuclei (Hoechst, white). Despite the nuclei being mispositioned in the *ens*^{swo} mutant, the mitochondria properly localize around the clustered nuclei. Therefore, any defect in the distribution of the mitochondria within the muscles is caused by the nuclear positioning defect in the *ens*^{swo} mutant larvae. Bar, 5 µm.

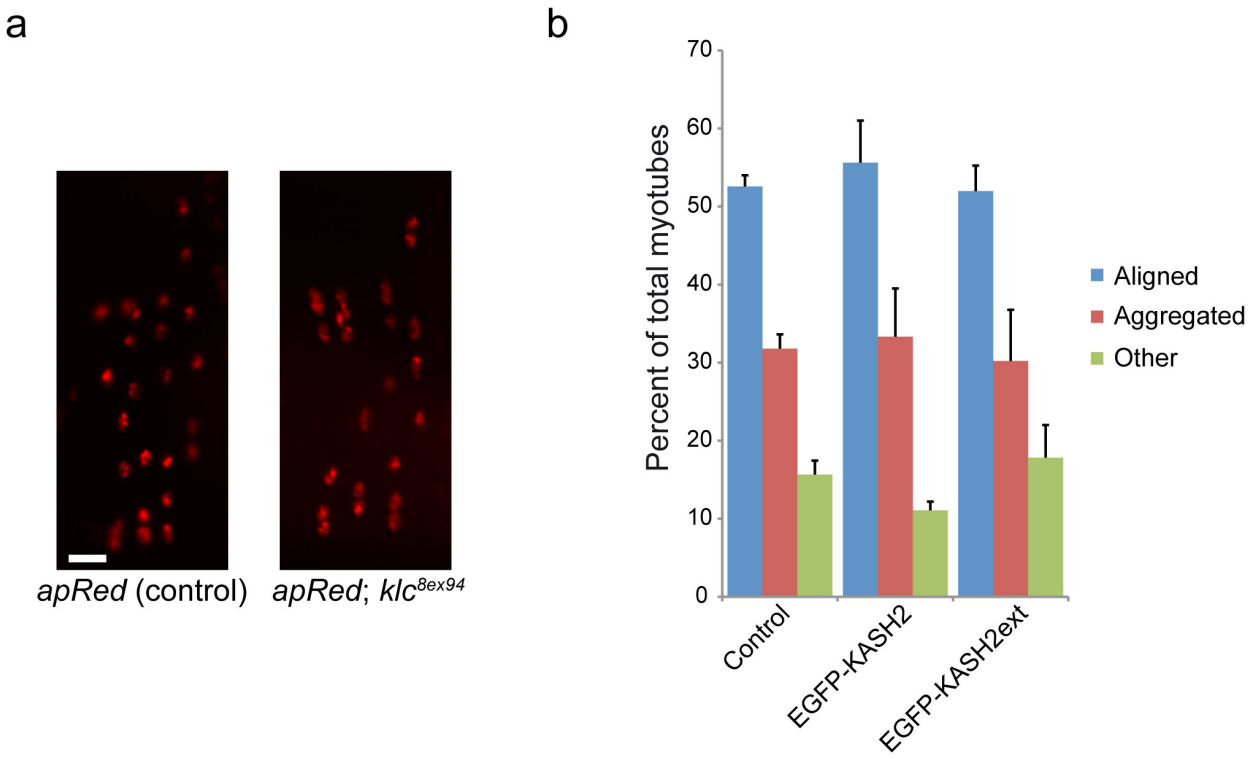

Supplementary Figure 9 | Kinesin light chain and KASH proteins are not required for nuclear migration in muscle. **a.** A single hemisegment from stage 17 *apRed* (control) and *apRed; klc*^{8ex94} mutant embryos, demonstrating that nuclei migrate and are properly spaced in *klc*-null mutant embryos. **b.** Histogram of nuclear position analysis in C2C12 myotubes in untreated (control) and in cells transfected with dominant-negative nesprin-2 KASH construct EGFP-KASH2 (which disrupts the LINC complex) and EGFP-KASH2ext (which does not disrupt the LINC complex)[38]. Error bars, s.e.m. Difference is not significant, $p > 0.1$.

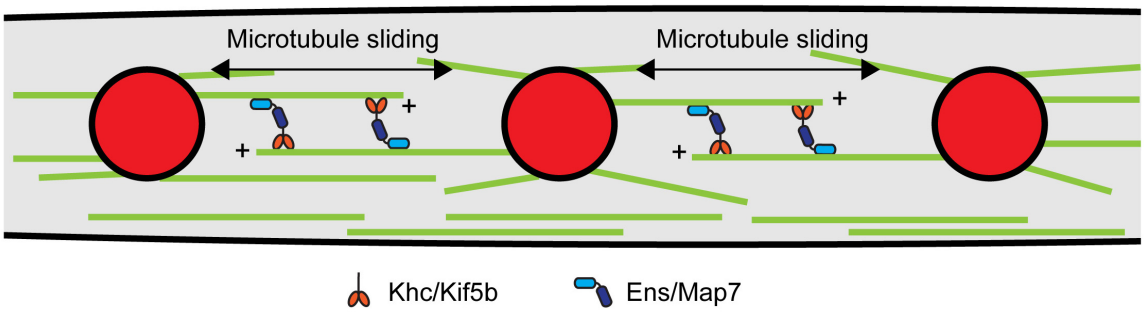

Supplementary Figure 10 | Model for nuclear positioning in muscle myofibers. In myotubes, most microtubules (green) in myofibers nucleate from and remain attached to the myonuclei (red). Thus, the microtubule networks from adjacent nuclei overlap forming anti-parallel arrays throughout the myofiber. Ens/Map7 (blue) forms a complex with Khc/Kif5b (orange) that can cross-link these anti-parallel microtubules. Movement of the Khc/Kif5b towards the plus end of one microtubule slides the anti-parallel Ens/Map7 bound microtubule relative to the first microtubule. Sliding of anti-parallel microtubules that are connected to adjacent nuclei thereby move the attached nuclei, resulting in the distribution of nuclei throughout the muscle.

Supplementary Movie 1 | Nuclear migration in the Lateral Transverse muscles of a wildtype *Drosophila* embryo. Movie of time-lapse sequence in Fig. 1b (top). Lateral view of a live *apME-NLS::dsRed* embryo where the nuclei of the Lateral Transverse (LT) muscles are labeled by the transgene (red). Time-lapse begins at stage 14 (11 h AEL, movie t = 0 h) when the nuclei in each muscle are clustered. The nuclei begin to separate into two distinct clusters, on dorsal and one ventral, during stage 15 (11.5 h AEL, t = 1.5 h) and the clusters are completely separated by stage 16 (15 h AEL, t = 3 h). During stage 17 (18 h AEL, t = 6 h) the nuclei within each cluster space and align into a single column within each muscle. Four columns of nuclei, one for each of the four LT muscles, are visible in each abdominal hemi-segment of the embryo.

Supplementary Movie 2 | Nuclear migration in the Lateral Transverse muscles of an *ens^{swo}* mutant embryo. Movie of time-lapse sequence in Fig. 1b (bottom). Lateral view of a live *ens^{swo},apRed* embryo where the nuclei of the Lateral Transverse (LT) muscles are labeled by the transgene (red). Time-lapse begins at stage 14 (11 h AEL, movie t = 0 h) when the nuclei in each muscle are clustered. The nuclei in an *ens^{swo}* mutant embryo never separate into the two distinct dorsal and ventral clusters. The nuclei remain as a single cluster until late stage 17 (18 h AEL, t = 6 h) when a small amount of separation can be observed. The columns of nuclei never fully extend in an *ens^{swo}* mutant embryo.

Supplementary Movie 3 | Control primary myotubes. Movie of time-lapse sequence in Supplemental Fig 4f (top) Control primary myotubes. Time: h.

Supplementary Movie 4 | *Map7* siRNA depleted primary myotubes. Movie of time-lapse sequence in Supplementary Figure 4f (bottom). *Map7* siRNA in primary myotubes. Time: h.

Supplementary Movie 5 | Control C2C12-H1B-GFP myotubes. Movie of time-lapse sequence in Fig. 1 (top). Control C2C12-H1B-GFP myotubes. Time: h.

Supplementary Movie 6 | *Map 7* siRNA C2C12-H1B-GFP myotubes. Movie of time-lapse sequence in Fig. 1d (bottom). *Map7* siRNA in C2C12-H1B-GFP myotubes. Time: h.

Supplementary Movie 7 | Control primary myotubes. Movie of time-lapse sequence in Supplementary Fig. 6f (left). Control primary myotubes. Time: h.

Supplementary Movie 8 | *Kif5b* siRNA depleted primary myotubes. Movie of time-lapse sequence in Supplementary Fig. 6f (right). *Kif5b* siRNA in primary myotubes. Time: h.